

# Screening subclinical keratoconus with Placido-based corneal indices

D. Ramos-López, A. Martínez-Finkelshtein, G. M. Castro-Luna, N. Burguera-Gimenez, A. Vega-Estrada, D.P. Piñero and J. L. Alió

Optometry & Vision Science

2013

This is **not** the published version of the paper, but a pre-print.  
Please follow the link below for the final version and cite this paper as:

D. Ramos-López, A. Martínez-Finkelshtein, G. M. Castro-Luna, N. Burguera-Gimenez, A. Vega-Estrada, D.P. Piñero and J. L. Alió. *Screening subclinical keratoconus with Placido-based corneal indices*. *Optometry & Vision Science*, Volume 90 (4), Pages 335-343, ISSN 1040-5488 (2013).

<http://dx.doi.org/10.1097/OPX.0b013e3182843f2a>

# **Screening subclinical keratoconus with Placido-based corneal indices**

Darío Ramos-López, MSc

Department of Statistics and Applied Mathematics, University of Almería, Spain

Andrei Martínez-Finkelshtein, PhD

Department of Statistics and Applied Mathematics, University of Almería, Spain and

Institute Carlos I of Theoretical and Computational Physics, Granada University, Spain.

Gracia M. Castro-Luna, MD, PhD

VISSUM Corporation, Almería, Spain

Neus Burguera-Gimenez, MSc

Keratoconus Unit. VISSUM Corporation, Alicante, Spain

Division of Ophthalmology, Universidad Miguel Hernández, Alicante, Spain

Alfredo Vega-Estrada, MD, MSc

Keratoconus Unit. VISSUM Corporation, Alicante, Spain

Division of Ophthalmology, Universidad Miguel Hernández, Alicante, Spain

David Piñero, PhD

Departamento de Óptica, Farmacología y Anatomía, Universidad de Alicante, Spain

Jorge L. Alió, MD, PhD

Keratoconus Unit. VISSUM Corporation, Alicante, Spain

Division of Ophthalmology, Universidad Miguel Hernández, Alicante, Spain

Address all correspondence to:

Andrei Martinez-Finkelshtein,

Department of Statistics and Applied Mathematics,

University of Almería, 04120 Almería, Spain;

Fax: +34950015167, e-mail: andrei@ual.es

This paper contains 6 Tables and 3 Figures.

Submitted on September 19, 2012

## **Abstract**

### **Purpose:**

To assess in a sample of normal, keratoconic and keratoconus suspect eyes the performance of a set of new topographic indices computed directly from the digitized images of the Placido rings.

### **Methods:**

This comparative study comprised a total of 124 eyes of 106 patients from the ophthalmic clinics Visum Alicante and Visum Almería (Spain), in three groups: control group (50 eyes), keratoconus group (50 eyes) and keratoconus suspect group (24 eyes). In all cases, a comprehensive examination was performed including the corneal topography with a Placido-based CSO topography system. Clinical outcomes were compared among groups, along with the discriminating performance of the proposed irregularity indices.

### **Results:**

Significant differences at level 0.05 were found on the values of the indices among groups by means of Mann-Witney-Wilcoxon non-parametric test and Fisher's exact test. Additional statistical methods, such as receiver operating characteristic analysis and K-fold cross-validation, confirmed the capability of the indices to discriminate between the three groups.

### **Conclusions:**

Direct analysis of the digitized images of the Placido mires projected on the cornea is a valid and effective tool for detection of corneal irregularities. Although based only on the data from the anterior surface of the cornea, the new indices performed well even when applied to the keratoconus suspect eyes. They have the advantage of simplicity of calculation combined with high sensitivity in corneal irregularity detection, and thus can

be used as supplementary criteria for diagnosing and grading keratoconus that can be added to the current keratometric classifications.

**Keywords:** Corneal irregularities; subclinical keratoconus; irregularity index; diagnosis; corneal topography; Placido disks

1 Keratoconus (KC) is an ectatic debilitating corneal disorder characterized by a  
2 progressive corneal thinning that results in corneal protrusion, irregular astigmatism, and  
3 decreased vision<sup>1</sup>. Corneal elasticity and rigidity is severely affected in keratoconic eyes<sup>2-4</sup>,  
4 which become more susceptible to the effect of any pressure, such as the intraocular pressure.  
5 Consequently, the corneal shape is more easily distorted (corneal steepening and aberrometric  
6 increase in KC). This explains the usual significant increase in the anterior corneal irregularity  
7 and a deterioration of the visual quality in KC, aggravated by the high optical relevance of the  
8 first surface of the cornea.

9 Several grading systems have been described in the literature in order to classify the  
10 severity of KC<sup>5-7</sup>. Most of these grading systems have been developed taking into account the  
11 visual performance of the patient, topographic morphology of the disease, the corneal  
12 keratometry readings and corneal aberrometry<sup>8-10</sup>, and have been proven to be an essential  
13 tool in the therapeutic approach to the management of KC.

14 Nevertheless, there is a form of this disease, characterized by a milder modification in  
15 corneal topography and morphology but without the impairment of the visual function of the  
16 patient, that has been defined as an early KC, subclinical KC, or KC suspect. One of the main  
17 difficulties in relation to this entity is the lack of its clear definition in the literature<sup>11</sup>.

18 The topographic analysis of the anterior corneal surface is the main tool that has been  
19 used for the KC diagnosis and characterization for years. Several indices, both simple and  
20 compound, decision trees and even neural networks based on the corneal topographic data and  
21 optical parameters have been developed to provide a more reliable tool to detect abnormal and  
22 borderline suspect corneas<sup>12-26</sup>. Also the vertical coma of the corneal aberration is one of the  
23 simplest direct KC markers used in the clinical practice<sup>9,13</sup>. However, and even with the  
24 advance of the technological tools employed today for the assessment of potential candidates  
25 for refractive surgery, subclinical KC is still considered the most important risk factor for

26 developing post LASIK ectasia<sup>27-28</sup>, a devastating condition leading to a significant visual  
27 impairment of the patient. Thus, improving the screening strategies, tools and techniques that  
28 allow us to identify those cases with the potential hazard of developing such a feared  
29 complication has become a major challenge within the ophthalmic community.

30 Most of the corneal indices, published in the literature, are based on the elevation or  
31 curvature data of the cornea, as well as pachymetry<sup>29</sup> or the epithelial thickness profile<sup>30</sup>.  
32 However, and at least in the case of the dominant Placido-based topographers, these data are  
33 not obtained by a direct (and verifiable) measurements, but are an outcome of a mathematical  
34 processing of the image of the rings in the keratographic picture by more or less sophisticated  
35 (and in the case of commercial devices, by proprietary and not always transparent)  
36 algorithms<sup>31-33</sup>. These procedures make important assumptions on the corneal shape  
37 (rotational symmetry, approximability by cubic splines, etc.) that are difficult to satisfy in the  
38 case of a very complicated or irregular corneal surface. Therefore, numerical approaches  
39 developed for KC detection from topographic data using these reconstruction algorithms  
40 inherit unnecessarily the complexity of the currently used ring image-to-curvature conversion  
41 methods, as well as might be affected by the unavoidable intrinsic errors appearing during  
42 such a conversion<sup>34-35</sup>.

43 In order to overcome these shortcomings, as well as to improve and complement the  
44 existing set of corneal disease markers, a set of new irregularity indices has been introduced  
45 recently<sup>36</sup>. These indices bypass the conversion to corneal power and use directly the digitized  
46 image of the Placido rings.

47 The previous contribution<sup>36</sup> had a methodological character, although some  
48 preliminary discussion of the performance of the indices was carried out there. The aim of this  
49 current study is to assess in a sample of normal, keratoconic and keratoconic suspect eyes a

50 simplified subset of the topographic indices proposed in that paper, evaluating their potential  
51 as a tool for KC detection.

52 As a final remark, we should point out that any additional information about a cornea,  
53 such as its pachymetry, could improve considerably the screening capability of any marker.  
54 The indices analysed here use only the data available to a Placido-based topographer (which  
55 are still a vast majority in the clinical practice), but we hope they help to use these data more  
56 efficiently.

57  
58

## Methods

59 This case series comparative study comprised a total of 124 eyes of 106 patients. Two  
60 Spanish ophthalmologic centers participated in the recruitment of patients for this study,  
61 Vissum Alicante and Vissum Almería, forming part of the Thematic Network of the  
62 Cooperative Sanitary Research (RETIC) RD07/0062. All these cases were assigned to one of  
63 the following three groups depending on the presence or not of KC: a control group, which  
64 included 50 eyes (from 50 patients), a KC group, which included a total of 50 eyes (from 32  
65 patients), and a subclinical KC or KC suspect group, with a total of 24 eyes (from 24  
66 patients).

67 The inclusion in the KC group was based on the standard criteria for the diagnosis of  
68 this corneal condition and the absence of any previous surgical intervention that could have  
69 altered the corneal properties. The following signs were considered at diagnosis<sup>1</sup>: corneal  
70 topography revealing an asymmetric bowtie pattern with or without skewed axes and at least  
71 one keratoconus sign on slit-lamp examination, such as stromal thinning, conical protrusion of  
72 the cornea at the apex, Fleischer ring, Vogt striae or anterior stromal scar. In those patients  
73 wearing contact lenses for the correction of the refractive error, only data obtained after an  
74 appropriate contact lens discontinuation were considered: at least 2 weeks for soft contact  
75 lenses and at least 4 weeks for rigid gas permeable contact lenses. The exclusion criteria for

76 the KC group were other ocular active pathology at the moment of diagnosis and the presence  
77 of an advanced KC (grade 4 according to the Alió-Shabayek grading system<sup>8</sup>). In cases of  
78 unilateral KC, the affected eye was always included in the study. However, in bilateral KC  
79 only one eye was selected randomly for the study.

80 The group of normal eyes or control group only included eyes with no other ocular  
81 pathology, previous ocular surgery or irregular corneal pattern. In this control group, only one  
82 eye from each patient was selected randomly (random sampling) for the inclusion in the study  
83 in order to avoid the potential bias introduced by the correlation between both eyes of a same  
84 patient.

85 The definition of KC suspect cases was based on the following clinical and  
86 topographic evaluation: no slit-lamp findings, no scissoring on retinoscopy, and the presence  
87 of asymmetric bowtie (AB), inferior steepening (IS), skewed axes (SRAX) or asymmetric  
88 bowtie with skewed axes (AB/SRAX) pattern on topography<sup>10</sup>.

89 All patients were informed about the study and signed an informed consent document  
90 in accordance with the Helsinki Declaration.

91

#### 92 *Examination protocol*

93 The corneal topographic analysis was carried out with the CSO topography system  
94 (CSO, Firenze, Italy). This topographer analyses a total of 6144 points of a corneal area  
95 enclosed in a circular annulus defined by an inner radius of 0.33 and an outer radius of 10 mm  
96 with respect to the corneal vertex. The software of this system, the EyeTop2005 (CSO,  
97 Firenze, Italy), performs automatically the conversion of the corneal elevation profile into  
98 corneal wavefront data using the Zernike polynomials with an expansion up to the 7<sup>th</sup> order,  
99 although it allows to export the raw data (positions of the digitized mires) as an ASCII file.  
100 For the sake of reliability of the analysis of the indices, the standard KPI index as well as the

101 I-S index has been stored for comparative purposes. Both indices are well known and  
102 precisely defined in the literature<sup>7,33</sup>.

103

#### 104 *Definitions of the corneal indices*

105 It is convenient to point out that in the description of the indices we skip the initial  
106 discretization step, performed by every commercially available topographer using presumably  
107 standard and widely available edge-detection procedures, when the high-contrast black-and-  
108 white images of the mires are converted into a discrete points set. Hence, we assume as the  
109 input data the coordinates of these points along the edges of consecutive mires, which we  
110 consider as positions of the digitized mires. With this information, we have calculated the  
111 irregularity indices following the previously discussed methodology<sup>36</sup>. From the original set  
112 of indices, we used a small subset of the best performing indices (also the most robust ones  
113 with respect to the misalignment of the eye and other errors), complemented with an  
114 additional index as described below.

115 The digitized points  $P_j$  captured by the camera of the Placido disk corneal  
116 topographer were grouped in  $N \in 15$  mires. For the sake of precision, we assume that there  
117 were 256 points equally spaced along each ring corresponding to the same number of semi-  
118 meridians (a value found in a majority of existing devices). We used only data from complete  
119 rings, limiting the number of rings to the maximum of 15. The indices were defined according  
120 to the information obtained from all mires as follows.

121

122 For each  $k$ , the center  $C_k$  and radius  $R_k$  of the best-fit circle for the  $k$ -th mire was  
123 calculated using a standard least squares procedure<sup>37</sup>, along with the following primary  
124 indices ( $PI$ ):

125  $-PI_1$ : the diameter of the set of centers  $C_k$  (normalized by the total number of rings  $N$ )

126 
$$PI_1 = \frac{1}{N} \max_{1 \leq n, m \leq N} \|C_n - C_m\|$$

127  $-PI_2$ : the total drift or the deviation in the consecutive centers  $C_k$ :

128 
$$PI_2 = \frac{1}{N-1} \sum_{1 \leq n \leq N-1} \|C_{n+1} - C_n\|$$

129 These two indices give global information about the deviation of the image of the  
 130 rings from a concentric pattern.

131 Data from mires were also fit with an ellipse with the aim of capturing the spatial  
 132 orientation and deformation of each mire (see Figure 1) by means of a simplification<sup>37-41</sup> of  
 133 efficient methods for computation of the best-fit ellipse, rendering the following asymmetry  
 134 index:

135  $-PI_3$ : the dispersion of the values of the axis ratios  $r_k = a_k/b_k \geq 1$  of the  $k$ -th best fit  
 136 ellipse by means of the following expressions:

137 
$$PI_3 = \sqrt{\frac{1}{N} \sum_{1 \leq k \leq N} (r_k - \bar{r})^2} \quad \text{where} \quad \bar{r} = \frac{1}{N} \sum_{1 \leq k \leq N} r_k$$

138 Indices  $PI_1 - PI_3$  coincide with those defined previously<sup>36</sup>. They were complemented  
 139 by some additional indices whose definition was modified with respect to that given  
 140 previously<sup>36</sup>, seeking better discrimination ability and robustness. In particular, we avoid the  
 141 use of polar coordinates (sensitive to the apex misalignment), calculating the indices  $AR(k)$   
 142 from the original image of the mires as the radius of the best-fit circle to the  $k$ -th ring. In  
 143 practice, only the fourth mire (index  $AR(4)$ ) was used in the combined model described  
 144 below, and thus only its individual performance will be analyzed in the next section.

145 We also carried out the standard linear regression of the coordinates of the centers  
 146  $C_k = (x_k, y_k)$ , yielding the coefficients for the linear fit  $y = ax + b$ . With this approach, high  
 147 values of  $a$  correspond to a vertical alignment of the centers, so its value contains information

148 about their spatial distribution (see Figure 2). These considerations motivate the following  
149 index (we use the name of an index defined previously<sup>36</sup>, but with a new meaning):

150  $-PI_4$ : is the absolute value of the slope of the linear regression,

$$151 \quad PI_4 = |a|$$

152 Each of these metrics can be used for KC detection (or at least, as a measure of  
153 corneal irregularity), but as it usually happens with the individual indices, none achieves the  
154 necessary sensitivity and specificity to meet the standards. For this reason, a combination was  
155 used to improve the detection efficiency. We added to our protocol of indices a new  
156 additional combined metric called GLPI, which takes continuous values between 0 and 100  
157 (0% corresponding to a totally normal, and 100%, to a totally altered cornea).

158 GLPI: is a generalized linear (Placido-based) model combining four of the individual  
159 indices mentioned above. Their linear combination (with fixed coefficients) is evaluated in  
160 the so-called "probit" link function<sup>42-43</sup>. This yields a quantity between 0 and 1 that is  
161 multiplied by 100 for convenience. This value, in the interval [0,100], is a % of irregularity of  
162 the cornea. This definition of GLPI is slightly different from the one given previously<sup>36</sup>: it has  
163 been modified to achieve a better accuracy with a smaller number of individual indices and  
164 also to include the redefined index  $PI_4$ :

$$165 \quad GLPI=100 \times \text{Probit}(\eta), \quad \text{with}$$

$$166 \quad \eta = 10^{-2}(15.7 + 1043.9 \times PI_1 - 184.2 \times PI_3 - 30.0 \times AR(4) + 0.5 \times PI_4) \quad (1)$$

167

### 168 *Statistical analysis*

169 In order to determine the homogeneity of the sample, when divided into training and  
170 test sets, a Mann-Witney-Wilcoxon non-parametric test<sup>44-45</sup> was applied to each of the  
171 primary indices. Without assumption of normality, this test checks whether the two samples

172 come from the same population (null hypothesis). It can also be used to analyze the  
173 discriminating ability of the indices, checking if it renders different values in each group.

174 Additionally, Fisher's exact test<sup>46-47</sup> is a statistical method used when a dichotomous  
175 classification process is made. This test checks whether the classifier has enough  
176 discrimination ability, and it is valid for any sample size. The idea is to compare the expected  
177 proportions of false/true positives/negatives with the actual proportion obtained after  
178 classifying. This procedure has been used in this study to check if the true proportions of  
179 success of the primary indices when classifying normal and keratoconic eyes are independent  
180 and consequently, if the primary indices show classification ability or not.

181 The K-fold cross-validation is a standard statistical tool to assess the global accuracy  
182 of a regression or classification model<sup>48-49</sup>. The main benefit of this method is that it makes  
183 use (independently) of the same data to fit the model and to check its performance, which is  
184 useful when the sample size is relatively small. The sample is divided into K groups of  
185 approximately equal size. Then the regression model is fit (or re-fit, if an initial model was  
186 specified) to the data using K-1 of the K subsets, and its accuracy is measured with the  
187 predicted values for the remaining group. When K becomes equal to the sample size, this  
188 scheme reduces to the well-known leave-one-out cross-validation method. This technique  
189 allows estimating the global accuracy of a classification method with only one dataset, but  
190 using independently subsets of the sample to fit and to validate the model.

191 Finally, the receiver operating characteristic (ROC) curve analysis is a well-  
192 established tool for assessing the discriminating capability of a model. We present the results  
193 of this analysis for the redefined primary indices  $PI_4$  and  $AR(4)$ . The ROC curves for the rest  
194 of the indices can be found in the literature<sup>36</sup>.

195

## Results

The primary indices have been computed for all three groups in the database and their means and standard deviations were calculated (see Table 1). The classification ability of the primary indices was assessed in different ways. First, according to the Mann-Witney-Wilcoxon tests, most of the indices are able to discriminate between the three groups (see Table 2), except for  $PI_2$  and  $AR(4)$ , which being appropriate for discrimination between keratoconic eyes (KC) and the rest of the eyes, do not perform well discriminating between normal (N) and keratoconus suspect (KS) eyes. In addition, Fisher's test for all these indices indicated that the true proportions of positives within the N and KC groups differ (with a significance level of 0.05), so they actually have sensitivity to detect irregularities. Moreover, the ROC curves for  $PI_4$  and  $AR(4)$  illustrate the discrimination ability of these indices (see Figure 3); the values of  $A_2ROC$  (area under the ROC curve) for all the indices appear on Table 2.

Concerning the combined indices, GLPI index computed using the whole database was able to reach the accuracy value 1 (perfect classifying capability between N and KC groups). The estimations rendered by the K-fold cross-validation method for different values of K are shown in Table 4, exhibiting consistent accuracy values between 0.94 and 0.95.

It is well known that the vertical coma (computed as the absolute value of the Zernike coefficient  $Z_3^{-1}$ ) is a simple marker for detecting  $KC^{9,13}$ . It is actually very close in spirit to our irregularity index  $PI_4$ : both measure the upper-down asymmetry, although  $PI_4$  follows the ideology of using only straightforward calculations from the mire images. For comparative reasons, the vertical coma has been also computed for all three groups in our database. According to a previous analysis<sup>36</sup>, a suitable cut-off value for the vertical coma to discriminate between keratoconus and normal eyes is  $3.59 \times 10^{-5}$ . With this threshold, 8% of the eyes in the KC group of our database were classified as regular and 4% of normal eyes

221 were classified as irregular, which is a good performance. However, within the keratoconus  
222 suspect group (KS), the vertical coma was able to classify only 29% of those corneas as  
223 irregular. To achieve a success rate of 0.79 within this group (the same as  $PI_4$ , see Table 6),  
224 the cut-off value has to be set approximately to  $2.00 \times 10^{-5}$ , yielding that 22% of normal eyes  
225 are classified as irregular. This is a much lower accuracy in comparison with  $PI_4$ .

226 There is a clear similarity in the philosophy of the construction of the KPI and the  
227 GLPI indices: both are compound indices, indicating a degree of certainty of detection of a  
228 corneal irregularity, with moderate to severe cones receiving a KPI score of 100%<sup>7, 50-51</sup>. Both  
229 indices are derived by a variation of discriminant analysis applied to a control group of  
230 patients, although GPLI, unlike the KPI, uses only the primary information provided by the  
231 keratoscope.

232 A comparison of the new indices with the KPI and I-S renders some interesting  
233 conclusions. For the keratoconus suspect group (KS) their values are summarized in Table 5.  
234 For the KPI, we used the standard cut-off reported in the literature, considering values equal  
235 to or greater than 23 as anomalous (the first two rows in Table 5 fall within the KPI range for  
236 normal eyes, while the last two rows correspond to anomalous ones); in the case of the I-S  
237 index, values equal or greater than 1.5 were considered anomalous (now, the first two  
238 columns in Table 5 correspond to normal eyes, according to the I-S index, and the last two  
239 columns correspond to anomalous eyes). It follows from Table 5 that KPI was able to detect  
240 only 6 out of 24 keratoconus suspect eyes (25%), while I-S was able to detect 12 out of 24  
241 (50%); moreover, 8 out of 24 cases were not detected by either indices (33.3%), and only 4  
242 out of 24 cases are detected by both indices simultaneously (16.7%).

243 Finally, Table 6 shows that the classification power of GLPI and KPI are very similar  
244 in all three groups: normal eyes, keratoconus eyes and keratoconus suspect eyes. Index  $PI_4$ ,  
245 exhibiting a reasonable behavior within the group of normal eyes, has a slightly lower KC

246 detection capability than either GLPI or KPI. However, within the crucial group of KS eyes,  
247 both GLPI (accuracy of 0.21) and KPI (accuracy of 0.29) have rather poor results, while the  
248 accuracy of PI<sub>4</sub> there is very acceptable (accuracy of 0.79).

249 This suggests the following clinical procedure to examine an individual eye. First, one  
250 computes GLPI (which has a high performance, close to the KPI's performance in all three  
251 groups) as the main diagnose tool. If the value of GLPI suggests a regular cornea, we look at  
252 PI<sub>4</sub>: if it renders values above the normal threshold of 1, we classify the patient as a possible  
253 keratoconus suspect, requiring further careful examination by the clinician before considering  
254 him/her as a candidate for, say, refractive surgery.

### 255 Discussion

256 The Placido-based anterior corneal topography is an affordable and valuable tool for  
257 screening for KC<sup>1</sup>. Moderate and advanced KC can be reliably diagnosed by this method,  
258 complemented with the biomicroscopic, retinoscopic and pachymetric study<sup>1</sup>. Much more  
259 challenging is the detection of this ectatic disorder in its very early or preclinical stages. In the  
260 last years, much effort has been devoted to improve the analysis of the corneal topography  
261 data in order to increase the ability to diagnose early clinical and subclinical KC cases. The  
262 importance of an early detection of such cases lies in particular in screening out the candidates  
263 for the refractive surgery procedures in these weakened and altered corneas. In this sense, a  
264 variety of indices or markers have been proposed in the last three decades. The most well-  
265 known and widely used ones are the Rabinowitz and Rabinowitz/McDonnell indices (K, I-S,  
266 KISA%), and the Klyce/Maeda indices (KPI, KCI%), along with the vertical coma<sup>9,13</sup>,  
267 although some others have also been defined<sup>33</sup>. Almost all of them, in accordance with the  
268 standard definition of KC, are based on a combination of pachymetry, curvature and corneal  
269 power maps obtained by means of corneal topography devices. However, at least in the  
270 devices based on Placido disk technology, the corneal power is not the directly measured

271 value but a product of a mathematical processing of the raw data, usually obtained under  
272 certain a priori assumptions and by proprietary methods, as explained above. This was one of  
273 the motivations for the introduction of new corneal irregularity indices<sup>36</sup> for the Placido disk  
274 topographers, defined and analyzed in this work. All of them use exclusively the primary  
275 data, that is, the image of the reflection of the mires on the anterior surface of the cornea,  
276 bypassing the need to calculate the altimetric or curvature data. It should be stressed that these  
277 new indices require only elementary arithmetic manipulation of the digitized images of the  
278 mires, and do not intend to imitate the reconstruction of the altimetry or local curvature of the  
279 cornea<sup>32</sup>. The aim of the current study was to evaluate in an available sample of normal,  
280 keratoconic and preclinical keratoconic eyes these new topographic indices derived directly  
281 from the analysis of the digitized images of the Placido rings, and to assess the potential of  
282 these indices as a tool for keratoconus detection. We insist that the primary purpose of our  
283 markers was not to replace but to complement the standard indices (KPI, KISA%, and others),  
284 eventually providing the clinician with an additional information, especially in the borderline  
285 and preclinical KC situations, by detecting an irregular cornea, independently of the type of  
286 irregularity it presents.

287         Regarding the primary corneal indices defined by our research group, statistically  
288 significant differences between the control and the KC groups were found for all indices.  
289 Therefore, the primary indices defining different features of the Placido disk images reflected  
290 on the cornea were able to discriminate between normal and KC corneas. A careful  
291 observation of the ranges of values of the primary indices in the analyzed groups reveals that  
292 there was a relevant area of overlapping for all parameter ranges of both groups. Therefore,  
293 these two primary indices showed the best discriminating ability among normal and KC eyes.  
294  $PI_2$  represents a measurement of the dispersion in the location of the centers of the fitted  
295 circles to the mires projected on the cornea, considering the diameter of the set of centers as

296 well as their drift<sup>32</sup>. Therefore, it characterizes the behavior of the centers of mass of each  
297 ring. The new  $PI_4$  is an indicator of the global asymmetry of the mires. Specifically, this index  
298 measures the slope of the regression line for the centers of the mires. In summary, the direct  
299 analysis of the asymmetry of the digitized Placido disks projected on the cornea by means of a  
300 corneal topography device allows an effective discrimination between normal and  
301 keratoconus corneas.

302 In the case of the combined index, an excellent discriminating performance of the  
303 GLPI (which can be interpreted as a percentage of irregularity) was observed. It was a perfect  
304 classifier between keratoconic and normal eyes, and yielded results comparable to the KPI  
305 when discriminating between the normal and subclinical KC eyes. Furthermore, a  
306 combination of GLPI with  $PI_4$  allows achieving an excellent capability of detection of  
307 irregular corneas, considering as irregular both the keratoconic and the preclinical keratoconic  
308 ones, as Table 6 shows. More specifically, all eyes in the KC group, as well as the majority of  
309 the eyes in the preclinical KC group, were classified by this combination of indices as  
310 irregular corneas. Thus, the use of the primary corneal indices characterizing the asymmetry  
311 of the mires seems to be especially useful for KC detection, while their combination yields a  
312 classification method with excellent discrimination ability between the three groups.

313 Along with the high sensitivity, another advantages of the corneal indices used in the  
314 current study over the standard approaches are (a) their independence from the proprietary  
315 algorithms of conversion of the raw ring images into curvature and corneal power, and (b) the  
316 mathematical simplicity, with consequent very basic computational requirements. It is  
317 convenient to remark that these indices can be easily adapted to any particular commercially  
318 available Placido disk topographer; keep in mind that these devices are simple, relatively  
319 affordable and easy to use, and represent a vast majority of the topographic devices available  
320 in the clinical practice.

321 We should point out also that the primary goal in the design of our markers was not  
322 the discrimination between types of pathology but rather a detection of irregularities on the  
323 anterior corneal surface. In this sense, we were not trying to replace the standard indices for  
324 the detection of KC (such as KPI, I-S or KISA%).

325 Currently, studies are being conducted in order to confirm the effectiveness of the  
326 defined indices in the detection and characterization of other corneal conditions. The  
327 correlation of these indices with higher order corneal aberrations and other optical quality  
328 parameters should be also investigated in the future.

329 In conclusion, the analysis of the digitized images of the Placido disks projected on  
330 the cornea is a valid and effective tool for the KC and preclinical KC screening that can be  
331 used additionally to the existing keratometric criteria. At this stage of our study, we can  
332 recommend them as a complementary screening tool designed to alert the clinician, especially  
333 in the borderline cases of irregular corneas for which a more exhaustive examination is  
334 recommended.

### 335 **Acknowledgments**

336 The authors have no proprietary or commercial interest in the medical devices that are  
337 involved in this manuscript. This study has been supported in part by the Thematic Network  
338 of the Cooperative Sanitary Research (RETIC) RD07/0062 from the Spanish Institute of  
339 Health "Carlos III". A.M.-F. and G.CdL are partially supported by the Research Project FIS  
340 PI10/01843 from the Spanish Institute of Health "Carlos III". A.M.-F. and D.R.-L. are also  
341 supported in part by the research group FQM-229 from Junta de Andalucía and by the project  
342 MTM2011-28952-C02-01 from the Ministry of Science and Innovation of Spain and the  
343 European Regional Development Fund (ERDF). Additionally, A.M.-F. is partially supported  
344 by the Excellence Grant P09-FQM-4643 from Junta de Andalucía.

345

346

347 **References:**

- 348 1. Rabinowitz YS. Keratoconus. *Surv Ophthalmol* 1998; 42:297-319.
- 349 2. Piñero DP, Alió JL, Barraquer RI, Michael R, Jiménez R. Corneal  
350 biomechanics, refraction, and corneal aberrometry in keratoconus: an  
351 integrated study. *Invest Ophthalmol Vis Sci* 2010; 51: 1948-55.
- 352 3. Shah S, Laiquzzaman M, Bhojwani R, Mantry S, Cunliffe I. Assessment of  
353 the biomechanical properties of the cornea with the Ocular Response  
354 Analyzer in normal and keratoconic eyes. *Invest Ophthalmol Vis Sci* 2007;  
355 48: 3026-31.
- 356 4. Ortiz D, Piñero D, Shabayek MH, Arnalich-Montiel F, Alió JL. Corneal  
357 biomechanical properties in normal, post-laser in situ keratomileusis, and  
358 keratoconic eyes. *J Cataract Refract Surg* 2007; 33: 1371-5.
- 359 5. Wilson SE and Klyce SD. Quantitative descriptors of corneal topography; a  
360 clinical study. *Arch of Ophthal*; 109: 349-53.
- 361 6. Maeda N, Klyce SD, Smolek MK. Comparison of methods for detecting  
362 keratoconus using videokeratography. *Arch of Ophthal*; 103: 870-74
- 363 7. Maeda N, Klyce SD, Smolek MK, Thompson HW. Automated keratoconus  
364 screening with corneal topography analysis. *Invest Ophthalmol Vis Sci*; 35:  
365 2749-57.
- 366 8. Alió JL, Piñero DP, Alesón A, Teus MA, et al. Keratoconus-integrated  
367 characterization considering anterior corneal aberrations, internal  
368 astigmatism, and corneal biomechanics. *J Cataract Refract Surg*. 2011;  
369 37:552-68.
- 370 9. Alió JL, Shabayek MH. Corneal higher order aberrations: a method to grade  
371 keratoconus. *J Refract Surg*. 2006 Jun;22(6):539-45.

- 372 10. de Rojas Silva V. Clasificación del Queratocono. In: Queratocono: pautas  
373 para su diagnóstico y tratamiento. Editor: Albertazzi R. Ediciones Científicas  
374 Argentinas para la Keratoconus Society, 2010: 33-97.
- 375 11. Li X, Yang H, Rabinowitz YS. Keratoconus: classification scheme based on  
376 videokeratography and clinical signs. J Cataract Refract Surg. 2009  
377 Sep;35(9):1597-603.
- 378 12. Ambrósio R, Belin MW. Imaging of the Cornea: Topography vs  
379 Tomography. J Refract Surg 2010;26(11):847-849.
- 380 13. Bühren J, Kühne C, Kohnen T. Defining subclinical keratoconus using  
381 corneal first surface higher-order aberrations. Am J Ophthalmol  
382 2007;143(3):381-389.
- 383 14. Saad A, Gatinel D. Topographic and Tomographic Properties of Forme Fruste  
384 Keratoconus Corneas. Invest Ophthalmol Vis Sci 2010;51(11):5546-5555.
- 385 15. Saad A, Lteif Y, Azan E, Gatinel D. Biomechanical Properties of  
386 Keratoconus Suspect Eyes. Invest Ophthalmol Vis Sci 2010;51(6):2912-  
387 2916.
- 388 16. Fontes BM, Ambrósio R, Velarde GC, Nosé W. Ocular Response Analyzer  
389 Measurements in Keratoconus with Normal Central Corneal Thickness  
390 Compared with Matched Normal Control Eyes. J Refract Surg  
391 2011;27(3):209-215.
- 392 17. Piñero DP, Alió JL, Alesón A, Escaf M, Miranda M. Pentacam posterior and  
393 anterior corneal aberrations in normal and keratoconic eyes. Clin Exp Optom  
394 2009; 92: 297-303.
- 395 18. Gobbe M, Guillon M. Corneal wavefront aberration measurements to detect  
396 keratoconus patients. Con Lens Anterior Eye 2005; 28: 57-66.

- 397 19. Barbero S, Marcos S, Merayo-Llodes J, Moreno-Barriuso E. Validation of the  
398 estimation of corneal aberrations from videokeratography in keratoconus. *J*  
399 *Refract Surg* 2002; 18: 263-70.
- 400 20. Carvalho LA. Preliminary results of neural networks and Zernike  
401 polynomials for classification of videokeratography maps. *Optom Vis Sci*  
402 2005; 82: 151-8.
- 403 21. Accardo PA, Pensiero S. Neural network-based system for early keratoconus  
404 detection from corneal topography. *J Biomed Inform* 2002; 35: 151-9.
- 405 22. Holladay JT. Corneal topography using the Holladay Diagnostic Summary. *J*  
406 *Cataract Refract Surg* 1997; 23: 209-21.
- 407 23. Borderie VM, Laroche L. Measurement of irregular astigmatism using  
408 semimeridian data from videokeratographs. *J Refract Surg* 1996; 12: 595-600.
- 409 24. Kalin NS, Maeda N, Klyce SD, Hargrave S, Wilson SE. Automated  
410 topographic screening for keratoconus in refractive surgery candidates.  
411 *CLAO J* 1996; 22: 164-7.
- 412 25. Rabinowitz YS, McDonnell PJ. Computer-assisted corneal topography in  
413 keratoconus. *Refract Corneal Surg* 1989; 5: 400-8.
- 414 26. Dingeldein SA, Klyce SD, Wilson SE. Quantitative descriptors of corneal  
415 shape derived from computer-assisted analysis of photokeratographs. *Refract*  
416 *Corneal Surg* 1989; 5: 372-8.
- 417 27. Randleman JB, Russell B, Ward MA, et al. Risk factors and prognosis for  
418 corneal ectasia after LASIK. *Ophthalmology* 2003;110(2):267-275.
- 419 28. Binder PS. Analysis of ectasia after laser in situ keratomileusis: risk factors. *J*  
420 *Cataract Refract Surg* 2007;33(9):1530-1538.

- 421 29. Prakash, G and Agarwal, A and Mazhari, A I and Kumar, G and Desai, P and  
422 Kumar, D A and Jacob, S and Agarwal, A. A new, pachymetry-based  
423 approach for diagnostic cutoffs for normal, suspect and keratoconic cornea.  
424 Eye 2012: 1-8.
- 425 30. Reinstein, D Z and Archer, T J and Gobbe, M, Corneal epithelial thickness  
426 profile in the diagnosis of keratoconus, J Refract Surg 25(7) 2009: 604-610.
- 427 31. Van Saarloos PP, Constable IJ. Improved method for calculation of corneal  
428 topography for any photokeratoscopic geometry. Optom Vis Sci 1991; 68:  
429 957-65.
- 430 32. Klein SA. A corneal topography algorithm that produces continuous  
431 curvature. Optom Vis Sci 1992; 69: 829-34.
- 432 33. Mahmoud AM, Roberts C, Lembach R, Herderick EE, McMahon TT; Clek  
433 Study Group. Simulation of machine-specific topographic indices for use  
434 across platforms. Optom Vis Sci 2006; 83: 682-93.
- 435 34. Greivenkamp JE, Mellinger MD, Snyder RW, Schwiegerling JT, Lowman  
436 AE, Miller JM. Comparison of Three Videokeratoscopes in Measurement of  
437 Toric Test Surfaces. J Ref Surg 1996; 12: 229-239.
- 438 35. Rand RH, Howland HC, Applegate RA. Mathematical model of a Placido  
439 disk keratometer and its implications for recovery of corneal topography.  
440 Optom Vis Sci 1997; 74: 926-930.
- 441 36. Ramos-López D, Martínez-Finkelshtein A, Castro-Luna GM, Piñero D, Alió  
442 JL. Placido-based indices of corneal irregularity. Optometry and Vision  
443 Science 88 (10) (2011), 1220-1231.

- 444 37. Ahn SJ, Rauh W, Warnecke HJ. Least-Squares Orthogonal Distances Fitting  
445 of Circle, Sphere, Ellipse, Hyperbola, and Parabola. *Pattern Recognition*  
446 2001; 34: 2283-303.
- 447 38. Mulchrone KF, Choudhury RK. Fitting an ellipse to an arbitrary shape:  
448 implications for strain analysis. *Journal of Structural Geology* 2004; 26: 143-  
449 53.
- 450 39. Halir R, Flusser J. Numerically stable direct least squares fitting of ellipses,  
451 Technical Report. Dept. Software Eng., Charles Univ., Czech Republic 2000.  
452 Available at: <http://library.utia.cas.cz/prace/980026.ps>. Accessed September  
453 17, 2012.
- 454 40. Fitzgibbon AW, Pilu M, Fisher RB. Direct least square fitting of ellipses.  
455 *IEEE Transactions on Pattern Analysis and Machine Intelligence* 1999; 21:  
456 476-80.
- 457 41. Hart D, Rudman AJ. Least-squares fit of an ellipse to anisotropic polar data:  
458 Application to azimuthal resistivity surveys in karst regions. *Computers &*  
459 *Geosciences* 1997; 23: 189-94.
- 460 42. McCullagh P, Nelder JA. *Generalized Linear Models*. 2<sup>nd</sup> edition. Boca  
461 Raton: Chapman & Hall/CRC; 1989.
- 462 43. Faraway JF. *Linear Models with R*. Boca Raton: Chapman & Hall/CRC;  
463 2005.
- 464 44. Bauer DF. Constructing confidence sets using rank statistics. *Journal of the*  
465 *American Statistical Association* 1972; 67: 687–690.
- 466 45. Hollander M, Wolfe DA. *Nonparametric Statistical Methods*. New York:  
467 John Wiley & Sons; 1973.

468 46. Agresti A. Categorical data analysis. Second edition. New York: Wiley;  
469 2001.

470 47. Fisher RA. Statistical Methods for Research Workers. Oliver & Boyd; 1970.

471 48. Picard R, Cook D. Cross-Validation of Regression Models. Journal of the  
472 American Statistical Association 1984; 79(387): 575–583.

473 49. McLachlan GJ, Do KA, Ambroise C. Analyzing microarray gene expression  
474 data. Wiley; 2004.

475 50. Burns DM, Johnston FM, Frazer DG, Patterson C, Jackson AJ. Keratoconus:  
476 an analysis of corneal asymmetry. Br J Ophthalmol. 2004; 88(10): 1252-  
477 1255.

478 51. Smolek MK, Klyce SD. Current keratoconus detection methods compared  
479 with a neural network approach, Invest Ophthalmol Vis Sci. 1997; 38(11):  
480 2290-2299.

481  
482  
483  
484  
485  
486  
487  
488  
489  
490  
491  
492  
493  
494  
495  
496

497 **Figure Legends**

498

499 Figure 1: An example of a digitized mire (dots) and its approximation by the best-fit-  
500 circle (left) and the best-fit-ellipse (right).

501

502 Figure 2: Centers  $C_k$  and the corresponding linear fit. Consecutive centers are  
503 connected in order to visualize better their relative drift, illustrating the different  
504 behaviors captured by indices  $PI_1$  (maximum distance) and  $PI_2$  (length of the path).

505

506 Figure 3: ROC curves for the redefined indices:  $PI_4$  (left) and  $AR(4)$  (right).

507

Table 1 – Mean and standard deviation values for the primary indices in the three groups in the database: Normal (N), Keratoconus (KC) and Keratoconus Suspect (KS).

<b>Primary Index</b>	<b>Normal group Mean (SD)</b>	<b>KC group Mean (SD)</b>	<b>KS group Mean (SD)</b>
<b>PI<sub>1</sub></b>	21 (16)	194 (131)	31 (16)
<b>PI<sub>2</sub></b>	28 (15)	166 (110)	27 (13)
<b>PI<sub>3</sub></b>	28 (17)	114 (90)	17 (13)
<b>PI<sub>4</sub></b>	29 (23)	208 (219)	100 (77)
<b>AR(4)</b>	34 (9)	55 (19)	52(9)

Table 2 – Summary of the non-parametric tests of equality of means between the three groups. All values in the table are P-values for the Mann-Witney-Wilcoxon test and \* meaning that significant differences (level 0.05) in the values of an index between groups were found.

<b>Primary Index</b>	<b>N vs KC</b>	<b>KC vs KS</b>	<b>N vs KS</b>
<b>PI<sub>1</sub></b>	< 0.01 *	< 0.01 *	< 0.01 *
<b>PI<sub>2</sub></b>	< 0.01 *	< 0.01 *	0.47
<b>PI<sub>3</sub></b>	< 0.01 *	< 0.01 *	< 0.01 *
<b>PI<sub>4</sub></b>	< 0.01 *	< 0.01 *	< 0.01 *
<b>AR(4)</b>	< 0.01 *	< 0.01 *	0.49

Table 3 – Value of the area under the ROC curve ( $A_z$ ROC) for the indices when classifying between regular eyes (normal group) and irregular eyes (keratoconus group).

<b>Index</b>	<b>PI<sub>1</sub></b>	<b>PI<sub>2</sub></b>	<b>PI<sub>3</sub></b>	<b>PI<sub>4</sub></b>	<b>AR(4)</b>	<b>GLPI</b>
<b>A<sub>z</sub>ROC</b>	0.987	0.989	0.880	0.936	0.837	1.000

Table 4 – Accuracy estimates (proportion of individuals well-classified) of the GLPI index defined in (1), for Normal and Keratoconus groups.

<b>Measurement</b>	<b>Accuracy value</b>
<b>5-fold</b> cross-validation accuracy estimate	0.95
<b>10-fold</b> cross-validation accuracy estimate	0.94
<b>Leave-one-out</b> cross-validation accuracy estimate	0.94

Table 5 – Joint frequency distributions for KPI and I-S values within the Keratoconus Suspect (KS) group. Each cell contains the number of KS eyes with a value of I-S within the interval at the top of that column and a value of KPI within the interval at the left of that row. Non-shaded cells correspond to those eyes diagnosed as normal eyes by both indices KPI and I-S. Light grey cells are the eyes classified as anomalous by one of these indices, whereas dark grey cells are the eyes screened as abnormal by both of them.

<b>KPI \ I-S</b>	<b>[-0.3, 0.4)</b>	<b>[0.4, 1.5)</b>	<b>[1.5, 2)</b>	<b>[2, 3]</b>
<b>[0,5)</b>	2	7	4	0
<b>[5, 23)</b>	0	2	2	1
<b>[23, 45)</b>	0	2	0	3
<b>[45, 55]</b>	0	0	0	1

Table 6 – Summary of results of classification ability of some of the proposed indices and the KPI. All the values within the table are the accuracy of each index when classifying in the stated group.

<b>Index</b>	<b>Normal</b>	<b>KC</b>	<b>KC Suspects</b>
<b>GLPI</b>	1.00	1.00	0.21
<b>KPI</b>	1.00	1.00	0.25
<b>PI<sub>4</sub></b>	0.87	0.90	0.79

Figure  
[Click here to download high resolution image](#)

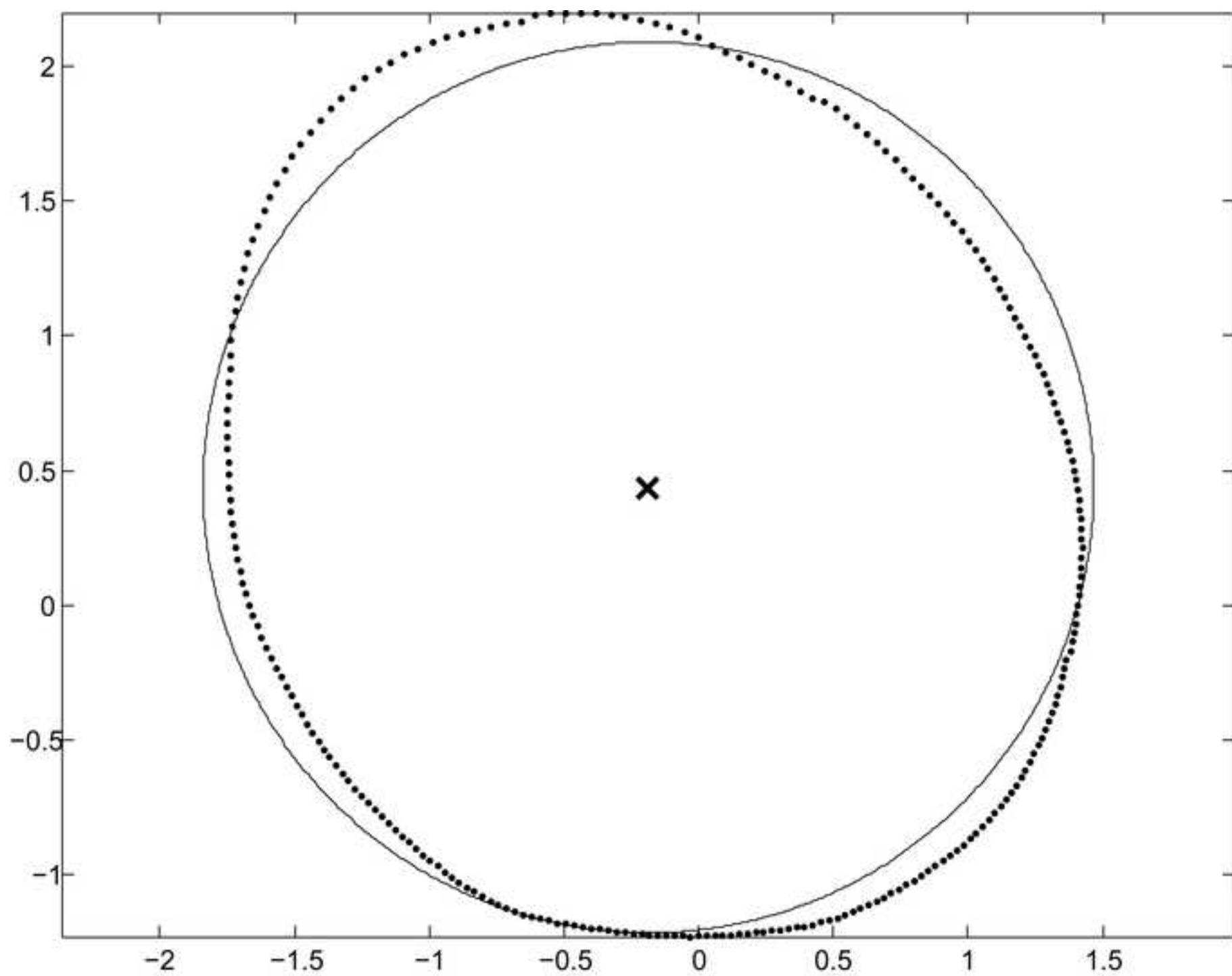


Figure  
[Click here to download high resolution image](#)

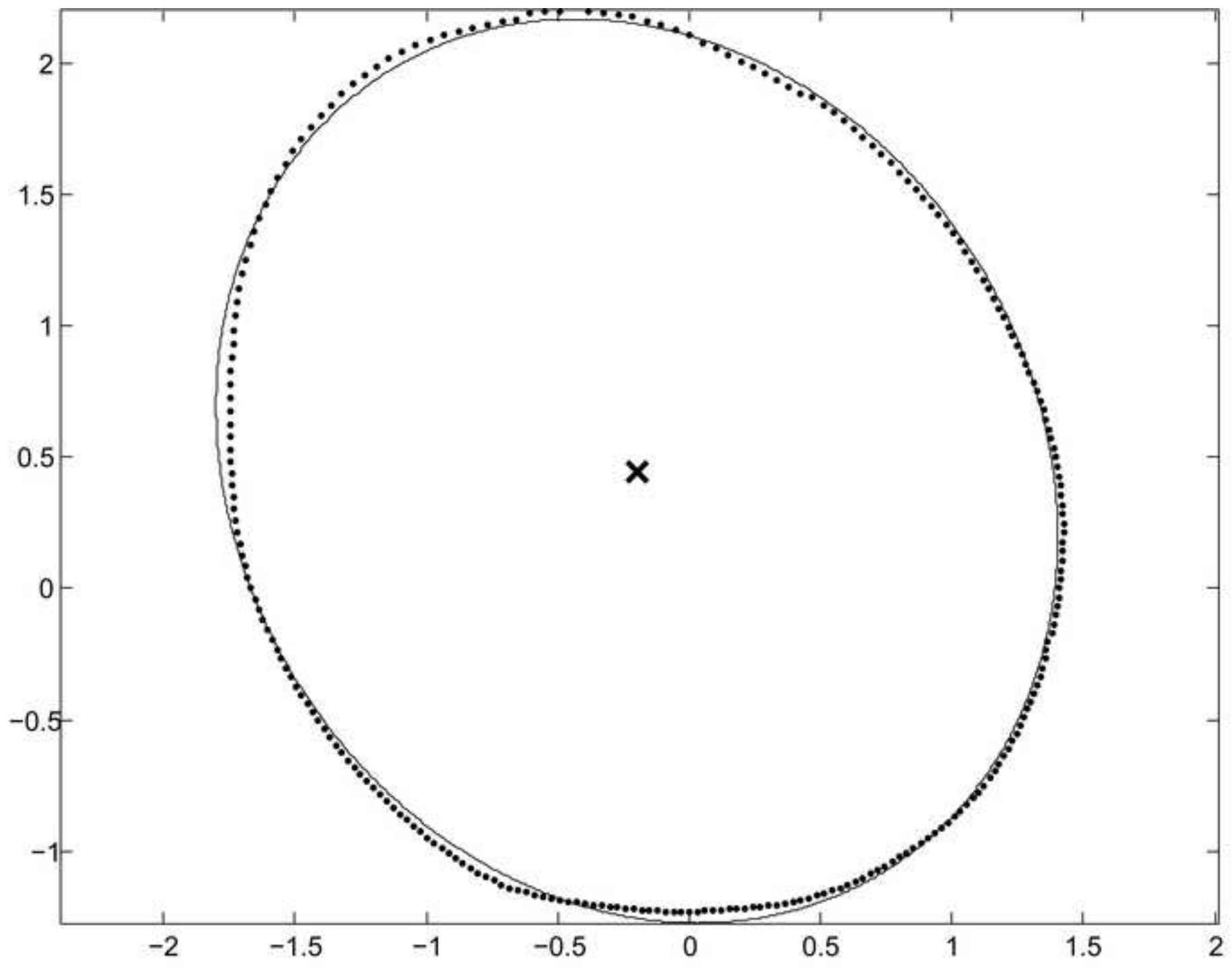


Figure  
[Click here to download high resolution image](#)

